

# The Laschamp geomagnetic dipole low expressed as a cosmogenic 10 Be atmospheric overproduction at 41 ka

L L Ménabréaz , Nicolas Thouveny, D L Bourlès, P Deschamps, B Hamelin,

F Demory

#### ► To cite this version:

L L Ménabréaz , Nicolas Thouveny, D L Bourlès, P Deschamps, B Hamelin, et al.. The Laschamp geomagnetic dipole low expressed as a cosmogenic 10 Be atmospheric overproduction at 41 ka. Earth and Planetary Science Letters, 2011, 312 (3-4), pp.305-317. 10.1016/j.epsl.2011.10.037 . hal-01420387

## HAL Id: hal-01420387 https://hal.science/hal-01420387v1

Submitted on 6 Feb 2017

**HAL** is a multi-disciplinary open access archive for the deposit and dissemination of scientific research documents, whether they are published or not. The documents may come from teaching and research institutions in France or abroad, or from public or private research centers. L'archive ouverte pluridisciplinaire **HAL**, est destinée au dépôt et à la diffusion de documents scientifiques de niveau recherche, publiés ou non, émanant des établissements d'enseignement et de recherche français ou étrangers, des laboratoires publics ou privés. 1 2

## The Laschamp geomagnetic dipole low expressed as a cosmogenic <sup>10</sup>Be atmospheric overproduction at ~41 ka.

- L. Ménabréaz, N. Thouveny, D.L. Bourlès, P. Deschamps, B. Hamelin and F. Demory.
- 5

6

7

Aix-Marseille Univ., CEREGE, BP80, 13545 Aix-en-Provence Cedex 04, France.
 CNRS, CEREGE, BP80, 13545 Aix-en-Provence Cedex 04, France.
 IRD, CEREGE, BP80, 13545 Aix-en-Provence Cedex 04, France.

#### 8 Abstract

9 Authigenic <sup>10</sup>Be/<sup>9</sup>Be ratio measurements were performed at high resolution along a Portuguese Margin deep-sea core (37°48 N; 10°09 W) spanning the 20-50 ka time interval, in 10 order to reconstruct variations in atmospheric cosmogenic <sup>10</sup>Be production rates and derive 11 the related geomagnetic dipole moment modulation. A complementary approach consisting in 12  $^{230}$ Th<sub>xs</sub>-normalized  $^{10}$ Be deposition rate determination on selected samples confirmed the 13 reliability of the authigenic <sup>10</sup>Be/<sup>9</sup>Be record. This study constitutes the first successful 14 comparison of the two widely-used normalization techniques of <sup>10</sup>Be concentrations. For both 15 16 methods, the presented results herein evidence a factor of ~2 cosmogenic nuclide 17 overproduction linked to a minimum dipole moment associated with the Laschamp 18 Excursion. The latter is stratigraphically constrained beneath Heinrich Event 4. Its age is 19 estimated at ~41 ka on the basis of direct correlation between the series of rapid paleoclimatic 20 events recorded in the Portuguese Margin sediments and in the Greenland ice sheet, and is 21 confirmed by calibrated radiocarbon dating carried out on the same sediments.

The remarkable agreement between the authigenic <sup>10</sup>Be/<sup>9</sup>Be and the Greenland Ice cores <sup>10</sup>Be deposition rate records attest to their global significance. This new authigenic <sup>10</sup>Be/<sup>9</sup>Be record has been combined with that previously obtained at the same site to produce a stacked record that is calibrated using absolute values of Virtual Dipole Moment determined on lava flows. This provides a reconstruction of dipole geomagnetic moment variations over the 20-50 ka interval, independent from paleomagnetically-constrained methods, that documents the Laschamp dipole low but fails to express any dipole low related to the Mono Lake Excursion.

This high resolution record responds to the necessity of supplementing the knowledge of the atmospheric  $\Delta^{14}$ C variations in the 30-45 ka interval during which the <sup>14</sup>C calibration curve suffers from a lack of accurate data, and during which a discrepancy of about 5500 yr between the <sup>14</sup>C and U-Th ages is due to the Laschamp geomagnetic dipole low. Such new high resolution datasets from records obtained from different latitudes will be required to make significant advances in understanding the causes of atmospheric  $\Delta^{14}$ C variations.

35

Key words: Cosmogenic nuclides; atmospheric <sup>10</sup>Be production rate; geomagnetic dipole
 moment; Laschamp Excursion; marine sediments.

38

#### 39 <u>1. Introduction</u>

The cosmogenic nuclide Beryllium-10 ( $^{10}$ Be, half-life: 1.387 ± 0.012 Ma (Chmeleff et 40 41 al., 2010; Korschinek et al., 2010)) is produced in the Earth's upper atmosphere by nuclear 42 interactions between energetic primary and secondary cosmic ray particles with target 43 elements O and N. As shown in the early work of Elsasser et al. (1956), and later refined by Lal (1988), <sup>10</sup>Be atmospheric production is directly modulated by the geomagnetic field 44 45 strength over millennial time scales, following a negative power law. This relationship 46 between the dipole moment and the atmospheric production rate of cosmogenic nuclides was 47 initially inferred from archeomagnetic absolute paleointensities and neutron monitor data 48 comparison (Elsasser et al., 1956). More recently, a physical model of cosmic ray particle 49 interactions with atmospheric targets yielded compatible simulations (Masarik and Beer, 50 1999; Wagner et al., 2000). Regarding the classically-used paleomagnetic reconstructions, <sup>10</sup>Be-derived paleointensity records can therefore constitute an alternative global and 51 52 independent reading of the dipole moment variations, and more particularly those that 53 accompany geomagnetic excursions and polarity events. During the last few years, efforts have been made to extract a geomagnetic signal from both single and stacked <sup>10</sup>Be records in 54 55 natural archives such as ice sheets (e.g. Muscheler et al., 2005) and marine sediments (e.g. 56 Frank et al., 1997; Carcaillet et al., 2004a; Christl et al., 2007). For these latter archives, two correction techniques were used to account for oceanic transport: the authigenic (adsorbed 57 from the water column) <sup>10</sup>Be/<sup>9</sup>Be ratio (Bourlès et al., 1989; Henken-Mellies et al., 1990; 58 59 Robinson et al., 1995; Carcaillet et al., 2003; Carcaillet et al., 2004a; Carcaillet et al., 2004b; Leduc et al., 2006) and <sup>230</sup>Th<sub>xs</sub>-normalisation (e.g. Frank et al., 1997; Christl et al., 2003; 60 Christl et al., 2007; Christl et al., 2010). The sole attempt to compare both correction 61 62 techniques was presented by Knudsen et al. (2008), but large uncertainties and environmental

63 complications prevented them from isolating the <sup>10</sup>Be production component from the 64  ${}^{10}\text{Be}/{}^{230}\text{Th}_{xs}$  signal.

65 The last 50 ka is a key period for the study and calibration of geomagnetic excursions and the associated cosmogenic responses, because this period contains the best-documented 66 67 and best-dated geomagnetic instability, the Laschamp Excursion (LE). This excursion was 68 first identified in the Laschamp and Olby lava flows of the Chaîne des Puys, France 69 (Bonhommet and Babkine, 1967), and was later described in lava flows of Iceland (e.g. 70 Kristjansson and Gudmundsson, 1980; Levi et al., 1990) and New Zealand (Cassata et al., 71 2008) notably. Other records of the Laschamp Excursion and/or associated dipole low were 72 obtained from lacustrine and marine sediments (e.g. Thouveny and Creer, 1992; Vlag et al., 73 1996; Lund et al., 2005; Channell, 2006). The most recent chronological constraints are provided by Ar-Ar, K-Ar, and <sup>230</sup>Th-U dating of lava flows from France (Laschamp, Olby and 74 75 Louchadière), and from New Zealand (McLennans Hill) (Guillou et al., 2004; Plenier et al., 76 2007; Singer et al., 2009). The statistical analyses of these age populations have led to the 77 following average ages:  $40.4\pm2.0$  ka (Guillou et al., 2004)  $40.7\pm1.0$  ka (Singer et al., 2009), 78 and 37.0±0.7 ka (Plenier et al., 2007), the third thus introducing a significantly younger age 79 estimation.

80 Another younger, but more controversial, excursion has also been documented: the 81 Mono Lake (ML) Excursion that was first detected in the Wilson Creek formation, California, 82 by Denham and Cox (1971) as they were seeking for a record of the Laschamp Excursion. It 83 was later described in other northwestern American lacustrine (e.g. Negrini et al., 1984; 84 Liddicoat, 1992; Coe and Liddicoat, 1994) as well as in marine sediments (e.g. Nowaczyk 85 and Knies, 2000; Channell, 2006). The radiometric age of the ML Excursion has been revised 86 from ~24 ka (Denham and Cox, 1971) to ~32 ka (Negrini et al., 2000; Benson et al., 2003). Surprisingly, other <sup>39</sup>Ar-<sup>40</sup>Ar dating of ash layers surrounding the excursion at Wilson Creek 87 88 (Kent et al., 2002) has yielded ages between 38 and 41 ka, which suggests that the excursion 89 recorded at Mono Lake could be the Laschamp Excursion. The correlation of the Mono Lake 90 RPI stack (Zimmerman et al., 2006) to the GLOPIS record of Laj et al. (2004) supported the 91 assignment of this excursion to the Laschamp. It remains true that most RPI records exhibit 92 two successive RPI lows at 32-34 ka and at 41 ka (e.g. Channel et al., 2006; Lund et al., 93 2005), which is also supported by recent reports of excursional directions and low absolute 94 paleointensities in lava flows at ages near 32 ka, i.e. distinct from the Laschamp age (Cassata 95 et al., 2008; Singer et al., 2009; Kissel et al., 2011).

96 The dipole field reduction linked to the Laschamp Excursion has been recorded as enhancements of <sup>10</sup>Be deposition rate in ice cores (e.g. Yiou et al., 1997; Muscheler et al., 97 2004; Raisbeck et al., 2007) and marine sediments (e.g. Frank et al., 1997; Christl et al., 2003; 98 99 Carcaillet et al., 2004b; Leduc et al., 2006). Regarding the ML Excursion, a Chlorine-36 100 atmospheric production enhancement detected at around 32 ka in the GRIP ice core (Wagner 101 et al., 2000) constitutes the only documented evidence for a significant increase of the 102 cosmogenic production. Atmospheric cosmogenic nuclide production variations induced by these geomagnetic instabilities need to be well constrained, notably because they impact <sup>14</sup>C 103 104 age calibration methods.

Here we present a highly resolved reconstruction of the <sup>10</sup>Be atmospheric production variations over the 20-50 ka interval, obtained from a well-dated 10 m sediment sequence deposited off the coast of Portugal. Authigenic <sup>10</sup>Be/<sup>9</sup>Be ratios were measured, and compared to <sup>230</sup>Th<sub>xs</sub>-derived <sup>10</sup>Be fluxes which were investigated on the same samples. The <sup>10</sup>Be production record was then transformed into a <sup>10</sup>Be-derived geomagnetic dipole moment record.

111

#### 112 2. Material and methods

#### 113 2.1 Coring site and sediment description

114 Climate and oceanographic settings as well as sedimentation processes within the area 115 have been described notably in Baas et al. (1997) and Pailler and Bard (2002). The sediment 116 deposition regime is related to glacial-interglacial sea-level variations and to the Tagus River 117 inputs. The contribution of large and variable continental material gave rise to a sediment 118 carbonate content of ~10% during glacials and ~50% during interglacials (Thomson et al., 119 1999; Hall and McCave, 2000), and with less than 1% organic matter (Pailler and Bard, 120 2002). Hemipelagic sediments along the Portuguese Margin also contain scarce and thin Ice 121 Rafted Debris (IRD) material diluted in the clay matrix (feldspars, quartz, magnetite and 122 hematite-coated grains). These layers detected by their IRD abundance and Magnetic 123 Susceptibility (MS) signatures have been shown to be contemporaneous with Heinrich Events 124 (Bard et al., 2000; Thouveny et al., 2000; Moreno et al., 2002).

Using different methodologies, several studies have demonstrated that the upper part of the giant cores collected with the Calypso corer of the R/V *Marion Dufresne* are affected by significant oversampling (e.g. Thouveny et al., 2000; Skinner and McCave, 2003 and Széréméta et al., 2004). This artefact has led to overestimations of apparent sedimentation rates (e.g. Thompson et al., 1999). Despite their perfect stratigraphic preservation, the upper l2 m of core MD95-2042 are affected by this artefact, which hampered the evaluation of accurate sedimentation rates and the interpretation of paleomagnetic and cosmogenic nuclides results.

133 During the MD-140 PRIVILEGE campaign of the R/V Marion Dufresne (2004) on the Portuguese Margin, a giant box corer CASQ  $(0.25m^2x12m)$  allowed to collect a high 134 135 resolution, undisturbed sediment sequence (Core MD04-2811; Lat.: 37°48 N; Long.: 10°09 136 W; 3162m water-depth) at the site of the previously studied SU81-18 and MD95-2042 cores 137 (Fig. 1; see references in caption). These cores were extensively studied for radiocarbon 138 calibration (section 3.2) and therefore benefits from an excellent chronological control. Core 139 MD04-2811 was thus selected in order to document a lack of the MD95-2042 record in the critical time interval (20-35 ka) and to assess accurate sediment fluxes using the  $^{230}$ Th<sub>xs</sub> 140 141 normalization.

MD04-2811 sediments are composed of oxidized carbonate-rich silty clays in the upper Holocene section (1.5m), and homogeneous hemipelagic silty clays deposited during the last glacial period.

#### 145 2.2 Paleomagnetic record and sampling strategy

Paleomagnetic investigations were performed on 1.5 m long U-channels collected along the MD04-2811 core. Low field Magnetic Susceptibility (MS) was measured using a Bartington MS2C probe. As described in former studies (e.g. Thouveny et al., 2000), the major structures of the MS profile consist in a succession of peaks corresponding to the ferrimagnetic responses of IRD layers deposited during Heinrich Events 1 to 5 superimposed on the paramagnetic contribution of the clayey fraction and a diamagnetic contribution of carbonates (Fig. 2).

Natural Remanent Magnetization (NRM) and artificially induced magnetizations were
measured using a 2G cryogenic magnetometer 760-SRM model and were demagnetized by
Alternating Fields (AF). The Relative Paleointensity (RPI) curve was established by
normalizing the NRM intensity to the Anhysteretic Remanent Magnetization (ARM)
intensity. The NRM/ARM ratio obtained for the 30mT AF demagnetization step (NRM<sub>30mT</sub>

158 /ARM<sub>30mT</sub>) represents the best estimate of the RPI. Three main RPI lows are recorded in the 159 435-520 cm, 575-630 cm and 740-810 cm intervals, the latter displaying the lowermost values 160 (Fig. 2). This structure is classically attributed to the dipole low related to the Laschamp 161 Excursion (e.g. Laj et al., 2004; Thouveny et al., 2004). The mean inclination of the 162 Characteristic Remanent Magnetizations equals ~  $50^{\circ}$ , i.e. it is weaker than the inclination 163 (56.8°) of the field created by a geomagnetic axial dipole field (GAD) at the site latitude. 164 Unlike other records of the area (Thouveny et al., 2004), there is no anomalous direction 165 related to the RPI low.

Based on the interpretation of the RPI profile, 52 sediment samples were taken at a 30 cm resolution, increased to 10 cm within paleointensity lows intervals, for <sup>10</sup>Be and <sup>9</sup>Be measurements.

#### 169 2.3 Analytical techniques

#### 170 *Leaching procedure: dissolution of the authigenic phase.*

In this study, authigenic <sup>10</sup>Be/<sup>9</sup>Be ratios, interpreted as a proxy of <sup>10</sup>Be fluxes, are 171 172 presented. Following the procedure thoroughly described in Bourlès et al. (1989), the 173 authigenic phase is extracted by leaching ~1g of dried and homogenized sediment using a 0.04M hydroxylamine in 25% acetic acid solution. A 2ml aliquot of the resulting leaching 174 175 solution is separated for natural <sup>9</sup>Be measurements. The remaining solution, spiked with 300µl of a 10<sup>-3</sup> g/g <sup>9</sup>Be-carrier, is used for chemical extraction and Accelerator Mass 176 Spectrometry (AMS) measurements of the resulting <sup>10</sup>Be/<sup>9</sup>Be ratio. This procedure permits to 177 178 overcome changes in extraction efficiency.

#### 179 *Total sample digestion and bulk sediment* <sup>10</sup>*Be content.*

<sup>230</sup>Th<sub>xs</sub>-normalized <sup>10</sup>Be flux quantification requires a total dissolution of sediment samples, assuming that lattice-bound <sup>10</sup>Be (from in-situ production) concentrations are negligible with respect to authigenic content. Sample dissolution was achieved at 70°C in a mixture of HF, HNO<sub>3</sub> and HCl (Bourlès et al., 1989), and spiked with 300 $\mu$ l of a 10<sup>-3</sup> g/g <sup>9</sup>Becarrier to perform chemical extraction and AMS measurements.

#### 185 Beryllium isotopes chemical extraction and measurements.

186 Once the sample is in solution, whatever the method used, Beryllium is then extracted 187 in the form of Be acetylacetonate using organic solvent. After decomposition of these 188 complexes, Be oxy-hydroxides are precipitated at pH 8 and oxidized to perform AMS 189 measurements at ASTER, the French AMS national facility (installed at the CEREGE) which 190 operates at 5MV. <sup>10</sup>Be concentrations are deduced from spiked <sup>10</sup>Be/<sup>9</sup>Be measured ratios 191 calibrated against the NIST 4325 Standard Reference Material with an assigned <sup>10</sup>Be/<sup>9</sup>Be 192 value of  $2.79 \times 10^{-11}$  (Nishiizumi et al., 2007), and are decay-corrected using the <sup>10</sup>Be half-life 193 of  $1.387 \pm 0.012$  Ma (Chmeleff et al., 2010; Korschinek et al., 2010):

194 
$$[{}^{10}Be]_{g/g}^{sample} = \left(\frac{{}^{10}Be}{{}^{9}Be}\right)_{M} \cdot \frac{m_{spike} \cdot [{}^{9}Be]_{spike}}{m_{sample}} \cdot e^{\lambda_{10} \cdot t}$$

195 where  $({}^{10}\text{Be}/{}^{9}\text{Be})_{\text{M}}$  is the measured Be ratio,  $\lambda_{10}$  is the decay constant of  ${}^{10}\text{Be}$  and  $m_{\text{sample}}$  is the 196 weight of the leached sediment powder sample.

197 Measured ratios as well as the resulting  ${}^{10}$ Be concentrations are listed in Table 1. 198 Chemistry blanks cluster around  $9 \times 10^{-15}$ , up to 1000 times lower than the  ${}^{10}$ Be/ ${}^{9}$ Be ratio of the 199 samples.

The external reproducibility obtained on the NIST SRM 4325 standard (estimated from 1 $\sigma$  standard deviation of long-term repeated measurements and integrating all effects contributing to the variability of ASTER) is limited to 0.6% (Arnold et al., 2010). Uncertainties in the measured <sup>10</sup>Be/<sup>9</sup>Be ratios and <sup>10</sup>Be concentrations were calculated from counting statistics and instrumental error propagation, according to the standard equation (e.g. Taylor, 1997).

Natural <sup>9</sup>Be concentrations were measured on the assigned 2ml aliquot using a 206 207 graphite-furnace Atomic Absorption Spectrophotometer with a Zeeman effect background 208 correction (Thermo Scientific ICE 3400) and the standard additions method (Table 1). Uncertainties in <sup>9</sup>Be concentrations depend on: (1) the reproducibility of the measured 209 absorbances at each added <sup>9</sup>Be concentrations (standard deviation less than 1%), and (2) the 210 least-square fitting between measured absorbances and added <sup>9</sup>Be concentrations ( $R^2$ >0.999). 211 212 Uncertainties (1 $\sigma$ ) in the <sup>9</sup>Be concentrations are generally significantly lower than 10% 213 (average value: 4.3%).

The final <sup>10</sup>Be/<sup>9</sup>Be uncertainty results from standard propagation of the above-cited <sup>10</sup>Be and <sup>9</sup>Be concentrations uncertainties. 216 Replicate authigenic <sup>10</sup>Be and <sup>9</sup>Be analyses were performed in order to check the 217 reproducibility of the Be isotopes chemical extraction (Table 1).

- 218 Uranium and Thorium isotopic analyses: chemical procedure and TIMS measurements.
- U-series measurements were performed by Thermo-ionisation Mass Spectrometry (TIMS) at the CEREGE) by using a  ${}^{236}U_{-}{}^{233}U_{-}{}^{229}$ Th mixed spike calibrated according to the procedure described in Deschamps et al. (2003).

222 The chemical procedure used to separate the uranium and thorium fractions for 223 determination of  ${}^{230}$ Th<sub>xs</sub> is similar to that described in Deschamps et al. (2004). Before total 224 digestion, samples were spiked. Total digestion was achieved by sequential treatments with 225 aqua regia and concentrated nitric and hydrofluoric acids. Following co-precipitation on iron 226 oxyhydroxides, U and Th fractions were chemically separated and purified using standard ion 227 exchange resins (AG-1X8 and U-Teva) and separation protocols modified from Deschamps et 228 al. (2004). Typical chemical blanks attained over the course of this study were about 0.25 ppb 229 for uranium and 0.28 ppb for thorium.

230 U and Th analyses were performed using a VG-Sector 54-30 mass spectrometer 231 equipped with a 30-cm electrostatic analyzer and an ion-counting Daly detector. The instrumental abundance sensitivity is greater than 0.15 ppm at 1 amu (proportion of the <sup>238</sup>U 232 233 ion beam measured at mass 237). The detailed procedure is described in Bard et al. (1990) 234 with further modifications described in Deschamps et al. (2011). U and Th fraction was 235 loaded on the side filament of a triple zone-refined Re filament assembly. Reported errors  $(2\sigma)$  for the <sup>234</sup>U/<sup>238</sup>U and <sup>230</sup>Th/<sup>232</sup>Th ratios are about 0.14 ‰ and 0.9 %, respectively. The 236 internal analytical reproducibility achieved in the course of this study on replicate 237 measurements of the NBS-960 international standard yielded a mean  $\delta^{234}$ U value of 238 239  $36.5\pm0.8\%$  (2 $\sigma$ , n=23) which is in excellent agreement with values reported in the literature 240 (Deschamps et al., 2003; Andersen et al., 2004).

To calculate excess <sup>230</sup>Th activity (<sup>230</sup>Th<sub>xs</sub>), measured <sup>230</sup>Th concentration is corrected for detrital and authigenic <sup>230</sup>Th components. The fraction of <sup>230</sup>Th supported by the decay of detrital <sup>238</sup>U is estimated from the <sup>232</sup>Th sample concentration and an assumed average lithogenic <sup>238</sup>U/<sup>232</sup>Th activity ratio of  $R = 0.6 \pm 0.1$  for the Atlantic Basin (Henderson and Anderson, 2003). Ingrowth of <sup>230</sup>Th from decay of authigenic uranium is estimated by assuming that authigenic uranium has an initial  ${}^{234}U/{}^{238}U$  activity ratio equivalent to that of sea-water (i.e. 1.147, Andersen et al., 2010).  ${}^{230}Th_{xs}$  activities were calculated as:

$${}^{230}Th_{xs} = {}^{230}Th_{Total} + R_{Crust} \times {}^{232}Th_{Total} \left( \left[ \left( \frac{234}{238}U \right)_0 - 1 \right] \times \frac{\lambda_{230}}{\lambda_{230} - \lambda_{234}} \left[ e^{-\lambda_{234} \times t} - e^{-\lambda_{230} \times t} \right] - e^{-\lambda_{230} \times t} \right) - {}^{238}U_{Total} \left( 1 - e^{-\lambda_{230} \times t} + \left[ \left( \frac{234}{238}U \right)_0 - 1 \right] \times \frac{\lambda_{230}}{\lambda_{230} - \lambda_{234}} \left[ e^{-\lambda_{234} \times t} - e^{-\lambda_{230} \times t} \right] \right)$$

where <sup>230</sup>Th<sub>Total</sub>, <sup>232</sup>Th<sub>Total</sub> and <sup>238</sup>U<sub>Total</sub> are the measured <sup>230Th</sup>, <sup>232</sup>Th and <sup>238</sup>U activities, respectively, and <sup>238</sup>U<sub>Total</sub>, is the sedimentary <sup>238</sup>U activity. (<sup>234</sup>U/<sup>238</sup>U)<sub>0</sub> stands for the initial (decay-corrected) authigenic activity ratio and the decay constants of radioisotopes i are expressed by  $\lambda_i$ .

The preserved, decay-corrected,  $^{230}$ Th<sub>xs</sub>-normalized  $^{10}$ Be deposition rates are then calculated following equations (11) and (12) as given in François et al. (2004), using a water depth of 3162 m.

Analytical errors and uncertainty related to assumption concerning the lithogenic  $^{238}U/^{232}$ Th activity ratio, R, were properly propagated through  $^{230}$ Th<sub>xs</sub> and flux calculations. Note that owing to small analytical errors achieved by the TIMS method, most of the final errors on  $^{230}$ Th<sub>xs</sub> and flux calculations are related to the arbitrary fixed uncertainty on R.

263

## 264 2.4 Using authigenic ${}^{10}Be/{}^{9}Be$ and ${}^{230}Th_{xs}$ -normalized ${}^{10}Be$ fluxes as tracers of geomagnetic 265 moment variations

The particle-reactive <sup>10</sup>Be is mainly produced in the atmosphere through nuclear 266 267 reactions (spallation reactions) on oxygen (O) and nitrogen (N), and is transferred to the 268 Earth's surface in soluble form by precipitation (Raisbeck et al., 1981) within ~3 yrs (Baroni et al., 2011). Atmospheric <sup>10</sup>Be is ultimately removed from water via settling particles and is 269 270 either deposited in marine and lacustrine sediments, or is efficiently retained by continental 271 sediment components, and finally enters the oceans through various paths and deposits in 272 deep sea sediments. Due to its short atmospheric residence time and chemical reactivity, <sup>10</sup>Be 273 records of production enhancements should be synchronous in the geophysical reservoirs. In marine sediments, the <sup>10</sup>Be concentration results from a complex interplay between several 274

275 processes: e.g. cosmogenic production, redistribution by atmospheric, riverine and oceanic 276 transport, adsorption and deposition processes. Considering the adsorption processes, for example, the absolute <sup>10</sup>Be concentration is controlled by the scavenging efficiency and the 277 278 specific surface of the settling sedimentary particles and thus depends on environmental 279 conditions affecting their chemical and grain size composition. Consequently, <sup>10</sup>Be 280 concentrations are meaningless and in order to account for these dependencies, a correction procedure is required. Soluble forms of <sup>10</sup>Be and <sup>9</sup>Be have different sources: while <sup>10</sup>Be is 281 cosmogenic, the stable isotope <sup>9</sup>Be originates from partial dissolution of detrital, aeolian and 282 283 riverine inputs (Brown et al., 1992). Once homogenized in seawater, both isotopes are 284 scavenged with the same efficiency. Authigenic <sup>10</sup>Be/<sup>9</sup>Be ratio of marine surface sediments reflects the Be isotope composition of the overlying deep waters, and its spatial variability is 285 286 mainly controlled by the proximity to continental <sup>9</sup>Be inputs (Bourlès et al., 1989). Although the authigenic <sup>9</sup>Be normalization method has provided promising results in specific 287 288 environments (Bourlès et al., 1989; Carcaillet et al., 2003; Carcaillet et al., 2004a; Carcaillet et al., 2004b; Lebatard et al., 2010), quantitative reconstructions of the <sup>10</sup>Be fluxes to the 289 290 sediment requires taking into account syndepositional lateral transport of adsorbed Be. Because residence time of Be in the water column is about 500-1000 yrs, boundary 291 292 scavenging and deepwater circulation must also contribute to the removal of dissolved Be and thus influence the <sup>10</sup>Be/<sup>9</sup>Be ratio. Moreover, lateral transport of adsorbed Be can be 293 294 significant in sediments heavily affected by focusing, such as drift deposits. However, at ocean margins where particle flux is high, the short Be residence time allows to record the 295 296 <sup>10</sup>Be atmospheric flux variations with almost no signal attenuation.

297 Assuming a scavenged flux equivalent to its known production rate in the overlying water column (Bacon, 1984), <sup>230</sup>Th can be used to quantify rates of particle rain to the 298 299 seafloor and to correct for syndepositional sediment redistribution by bottom currents. The 300 principles and limitations of this method are fully reviewed in Henderson and Anderson (2003) and François et al. (2004). Like authigenic  ${}^{10}\text{Be}/{}^{9}\text{Be}$ , the  ${}^{10}\text{Be}/{}^{230}\text{Th}_{xs}$  ratio may also be 301 potentially influenced by advection of dissolved Be. Moreover, biases resulting from nuclide 302 303 characteristics (different chemical affinities) are introduced: one illustration of this problem is 304 reported by Chase et al. (2002), who showed a composition-dependant differential scavenging 305 of Be and Th, suggesting that opal/carbonate ratio of settling particles may partly explain the sedimentary  ${}^{10}\text{Be}/{}^{230}\text{Th}_{xs}$  variability. 306

307 Here, authigenic  ${}^{10}\text{Be}/{}^9\text{Be}$  ratios were measured for 51 sampled layers, and an 308 additional  ${}^{230}\text{Th}_{xs}$ -normalization was performed for 9 of them, which were selected using the 309 Be isotopes ratio profile. This allows direct comparison and cross-calibration on the same 310 homogenized material.

311 3. Results

### 312 3.1 The authigenic <sup>10</sup>Be/<sup>9</sup>Be ratios and RPI on the same sequence

Authigenic <sup>9</sup>Be concentrations vary from  $4.35 \times 10^{-7}$  g/g to  $7.22 \times 10^{-7}$  g/g (Table 1), 313 refining and confirming the previous range obtained on adjacent core MD95 2042 by 314 Carcaillet et al. (2004). Decay-corrected authigenic <sup>10</sup>Be concentrations vary around a mean 315 value of  $7.32 \times 10^{-15}$  g/g with a prominent increase to  $13.6 \times 10^{-15}$  g/g at 712 cm. The range of 316 variation (5.33 to  $13.6 \times 10^{-15}$  g/g) and the average value are identical to those of the adjacent 317 318 core MD95 2042 (Carcaillet et al., 2004b). The resulting authigenic <sup>10</sup>Be/<sup>9</sup>Be evolution is 319 presented in Figure 2, and compared to the RPI and MS profiles. The main feature of the <sup>10</sup>Be/<sup>9</sup>Be record is a unique significant enhancement at 712 cm, with <sup>10</sup>Be concentrations 320 leading to a near doubling of the long-term average  ${}^{10}\text{Be}/{}^{9}\text{Be}$  value of  $1.44 \times 10^{-8}$  to  $2.69 \times 10^{-8}$ . 321

Along this sequence, both records of the <sup>10</sup>Be atmospheric production and its geomagnetic modulation display inverse long-term trends. While the RPI record exhibits three minima, only one significant enhancement appears in the <sup>10</sup>Be/<sup>9</sup>Be record, with values above the "mean+1 $\sigma$ " occurring between 662 and 722 cm depth. This interval overlaps the depth interval recording the lowest RPI values located between ~690 and ~820 cm. The depth shift thus evidenced between these two expressions of the dipole low is further discussed in section 4.1

#### 329 3.2 Chronostratigraphy

The first step in establishing the chronostratigraphy of core MD04-2811 is to construct a correlation matrix based on the MS records (Fig. 3) with the dated neighboring core MD95 2042 (Lat.: 37°45'N; Long.: 10°10'W; 3146 m water depth) in order to translate the available chronological data onto the MD04-2811 depth scale (Fig. 4).

Two major studies have established radiocarbon dates series on MD95-2042 (Bard et al., 2004; Shackleton et al., 2004, Electronic Appendix, Table A.1) that were compared with ages obtained from correlations with annually laminated Greenland ice cores (GRIP and GISP2). Among the paleoclimatic proxies measured along the MD95-2042 sequence, seasurface temperature proxies (alkenones and planktonic  $\delta^{18}$ O) show marked variations which are in robust mutual stratigraphic agreement, and which correlate to Dansgaard-Oeschger cycles and Heinrich Events. For this study, the age control on the core MD95-2042 was updated by tuning the alkenone-derived sea-surface temperature record with the NGRIP oxygen isotopes record using a minimum number of tie points (R= 0.876, Fig. 3 and 4).

343 Uncertainties affecting the age model are derived from the two-sigma GICC05 time-344 scale uncertainties associated with multi parameter counting of annual layers (Andersen et al., 345 2006; Rasmussen et al., 2006): the glacial part of this time scale has an estimated associated 346 error of 2% back to 40 ka and of 5-10% back to 57 ka. Although multiple correlation 347 procedures - limited by precision and resolution of the individual time series - and the 348 accuracy of the cross-correlation procedure represent a source of uncertainty which is difficult 349 to quantify using simple statistical parameters, the computed age model is validated by the fact that the ages assigned to the Heinrich Events (Fig. 4) are indistinguishable from the 350 calibrated <sup>14</sup>C ages obtained on North Atlantic basin sediment sequences (Thouveny et al., 351 352 2000). Moreover, the <sup>14</sup>C ages obtained on the studied sequence calibrated using the INTCAL09 dataset (Reimer et al., 2009) relying mainly on  $^{234}$ U/ $^{230}$ Th absolute dating of Hulu 353 354 Cave stalagmites (China, Wang et al., 2001) over the 35-45 ka period (Electronic Appendix, 355 Table A.1) are fully compatible with this ice core-derived chronology.

## 356 3.3 <sup>10</sup>Be deposition rates (excess <sup>230</sup>Th-normalized <sup>10</sup>Be fluxes)

Bulk <sup>10</sup>Be concentrations obtained after total sample dissolution are comprised 357 between  $1.1 \times 10^{-14}$  g/g and  $1.8 \times 10^{-14}$  g/g (see Table 2). Total mass flux ranges between 4.79 358 and 6.09 g/cm<sup>2</sup>/ka, and is fully compatible with results obtained further northward on the 359 360 Portuguese Margin by Thomson et al. (1999), who determine a total sediment accumulation flux of ~5 g/cm<sup>2</sup>/ka during glacial times over the last 140 ka. Preserved vertical  $^{10}$ Be 361 deposition rates vary from  $3.18 \times 10^9$  to  $6.59 \times 10^9$  atoms/cm<sup>2</sup>/ka (Fig. 5a). The <sup>10</sup>Be deposition 362 rate downcore evolution is strictly similar to that of the authigenic <sup>10</sup>Be/<sup>9</sup>Be ratios measured 363 364 on the same samples: the characteristic increase with a maximum at 712 cm depth is indeed reflected in the <sup>10</sup>Be deposition rates record. The comparison between authigenic <sup>10</sup>Be/<sup>9</sup>Be 365 ratios and <sup>230</sup>Th<sub>xs</sub>-normalized <sup>10</sup>Be fluxes is illustrated in Figure 5b. The linear relationship 366 367 between these two variables is highly significant (R = 0.912), albeit mainly carried by the 368 maximum variability recorded during the main enhancement.

#### 370 4. Discussion

#### 371 4.1 Identification of the Laschamp dipole low and chronological implications

372 During low dipole field intervals, the magnetic torqueses are insufficient to align 373 magnetic grains and so ensure acquisition of a well-defined magnetization. Nevertheless, after 374 recovery of the field strength, re-alignments of magnetic grains and acquisition of viscous 375 magnetization (VRM) result in a biased record of directions and intensities (e.g. Coe and 376 Liddicoat, 1994). In core MD04-2811, as in other neighboring cores (see Figures 4 and 9 in 377 Thouveny et al., 2004), the structure of paleomagnetic records (directions and RPI) does not 378 allow an accurate and precise stratigraphic positioning of the dipole field minimum. 379 Comparison of the positions of the respective boundaries of the main RPI low (at ~700 and ~820 cm) with the main  ${}^{10}\text{Be}/{}^9\text{Be}$  enhancement (at ~660 cm and ~725 cm) calls attention to a 380 381 ~50 cm lag between the two signals (Fig. 2). This lag integrates a maximum 10 cm shift due 382 to the residence time with respect to scavenging of Be, given a ~1 cm/50 yrs average 383 sedimentation rate. The remaining 40 cm lag is greater than the 15-30 cm lags revealed from 384 neighboring cores by Carcaillet et al. (2004); however given the sources of distortions cited 385 above, it is not possible to assign this lag to the magnetization lock-in depth only.

386 In core MD95-2042 core, the declination anomaly and the RPI low related to the 387 Laschamp excursion are recorded 50 cm beneath the MS peak associated with the Heinrich 388 Event 4 (Thouveny et al., 2004). In North Atlantic Ocean cores (Kissel et al., 1999), 389 excursional inclination peaks related to the Laschamp are recorded at the same stratigraphic 390 position as rock-magnetic signatures of the Dansgaard-Oeschger (D-O) Interstadial 10, i.e 391 prior to H4. Nevertheless, the best stratigraphic indicator of the occurrence of the dipole low 392 related to the Laschamp is the cosmogenic nuclide signature which is not affected by delays 393 and distortions imparted by post-depositional processes.

Along core MD04-2811 the highest  ${}^{10}$ Be/ ${}^{9}$ Be ratio peak - recorded ~40 cm beneath the 394 MS peak corresponding to H4 - can thus undoubtedly be interpreted as the <sup>10</sup>Be atmospheric 395 396 overproduction due to the geomagnetic dipole reduction associated with the Laschamp 397 Excursion (LE). This 40 cm depth interval suggests that the LE occurred ~2 ka before 398 Heinrich Event 4, which is dated at ~39 ka in North Atlantic sedimentary sequences (e.g. Thouveny et al., 2000). Indeed, the chronological reconstruction positions the <sup>10</sup>Be/<sup>9</sup>Be 399 400 Laschamp signature at  $41.2 \pm 1.6$  ka (minimal uncertainty derived from GICC05 chronology). 401 This age is coherent with the most recent independent radiometric age determinations obtained on volcanic material ( $40.4 \pm 2.0$  ka, Guillou et al., 2004;  $40.7 \pm 0.9$  ka, Singer et al., 2009). It also coincides tightly with the age of the maximum <sup>10</sup>Be flux in Summit ice cores (Muscheler et al., 2005; Svensson et al., 2008). This suggests that the <sup>10</sup>Be residence time in the water column in such settings is short enough to preserve the simultaneity of the record in both geological reservoirs, considering age uncertainties and resolution.

The <sup>10</sup>Be production and recording processes in sedimentary sequences that are totally 407 408 independent from: 1) the local geomagnetic vector, and 2) magnetization processes in weak 409 and highly variable local fields, enable to evaluate the duration of the dipole field anomaly. 410 Both the high resolution and the accurate dating of this record highlight the persistence of a weak dipole field defined by authigenic  ${}^{10}\text{Be}/{}^{9}\text{Be}$  values above "mean+1 $\sigma$ " during ~2.5 ka. 411 The minimum field intensity phase defined by authigenic  ${}^{10}\text{Be}/{}^{9}\text{Be}$  values above "mean+2 $\sigma$ " 412 413 lasted about 1 ka. This duration estimate is similar to that provided by the ice core record of 414 Muscheler et al. (2005).

## 415 **4.2** Significance of the <sup>10</sup>Be/<sup>9</sup>Be record

## 416 ${}^{10}Be/{}^{9}Be$ ratios and ${}^{230}Th_{xs}$ -normalized ${}^{10}Be$ fluxes: a cross evaluation

In this study, <sup>10</sup>Be deposition rates reinforce the authigenic <sup>10</sup>Be/<sup>9</sup>Be signal validity. 417 Comparison between the amplitude of <sup>10</sup>Be/<sup>230</sup>Th<sub>xs</sub> and authigenic <sup>10</sup>Be/<sup>9</sup>Be variations shows 418 419 that both records agree within uncertainties (Fig. 6a) and document an increase by a factor of 420 ~2 coincidental with the Laschamp geomagnetic dipole low. This is the first time that such a 421 match has been reported, demonstrating that both normalization methods provide equivalent results in this case, and that normalizing authigenic <sup>10</sup>Be concentrations by authigenic <sup>9</sup>Be 422 423 concentrations allows a reliable correction for total particle flux variations. Moreover, quantification of the vertical <sup>10</sup>Be fluxes allows to underline the effects of boundary 424 scavenging: the <sup>10</sup>Be deposition rates determined in this study (mean value:  $4.09 \pm 0.31 \times 10^9$ 425 at./cm<sup>2</sup>/ka) are (1) both slightly higher than an estimate of the present global production rate 426 of  $1.21 \pm 0.26 \times 10^9$  at./cm<sup>2</sup>/ka (Monaghan et al., 1986) and higher than Greenland <sup>10</sup>Be fluxes 427 428  $(0.25 \text{ to } 0.6 \times 10^9 \text{ at./cm}^2/\text{ka}$  (Muscheler et al., 2004)); and (2) within the range reported for Atlantic drift deposits of the last 75 ka (~1 to  $7x10^9$  at./cm<sup>2</sup>/ka, Christl et al., 2007; Knudsen et 429 al., 2008; Christl et al., 2010). Although the resolution of the  ${}^{10}\text{Be}/{}^{230}\text{Th}_{xs}$  record must be 430 improved, the observed close agreement suggests that the effects of rapid millennial-scale 431 432 changes in deep water circulation (advection of dissolved Be and Th) could be either similar 433 in both approaches, or insignificant.

434 Comparison with <sup>10</sup>Be production rate ice core records and with relative geomagnetic field
435 intensity reconstructed from paleomagnetic records

436 Over the 20-50 ka interval, there is a remarkable match between the MD04-2811 authigenic <sup>10</sup>Be/<sup>9</sup>Be record and the <sup>10</sup>Be flux variations recorded along the GRIP and GISP2 437 438 ice cores (Fig. 6b; Finkel and Nishiizumi, 1997; Yiou et al., 1997; Muscheler et al., 2005). It 439 must be emphasized that even small variations of the two records match which strongly supports the high quality of the authigenic <sup>10</sup>Be/<sup>9</sup>Be record presented. Observed for such 440 441 different geophysical reservoirs as marine sediments and polar ice, this agreement demonstrates that this ratio most likely mainly reflects the changes in global atmospheric <sup>10</sup>Be 442 production rate. This confirms that the normalization of authigenic <sup>10</sup>Be concentrations to 443 authigenic <sup>9</sup>Be concentrations minimizes the impact of secondary mechanisms, among which 444 445 ocean system effects (see section 2.4). In addition, the fact that these variations are recorded with the same amplitude in both archives, indicates that the <sup>10</sup>Be residence time in the 446 447 atmosphere-ocean reservoirs should be short enough to minimize the attenuation of the production signal. The Laschamp signature corresponds to the near-doubling of the global 448 449 atmospheric <sup>10</sup>Be production expected from the physically constrained algorithm (Elsasser et al., 1956; Lal, 1988) which expresses the control of global atmospheric <sup>10</sup>Be production rate 450 451 exerted by the magnetospheric shielding as modulated by geomagnetic moment variations,. This also suggests that a significant component of the Greenland <sup>10</sup>Be flux signal results from 452 453 an atmospheric transport from lower latitudes. Another important result is that these marine and ice core records of the atmospheric <sup>10</sup>Be production rates both fail to display any other 454 significant <sup>10</sup>Be deposition enhancement. Wagner et al. (2000a) identified in the GRIP ice 455 core an increased <sup>36</sup>Cl flux between D-O events 6 and 7, which they attributed to the RPI 456 457 minimum observed at ~34 ka in the NAPIS-75 stack (based on the GISP-2 chronology; Laj et 458 al., 2000), and referred to as the Mono Lake Excursion. After smoothing of the dataset with a 1/2000 yrs<sup>-1</sup> low-pass filter, the <sup>36</sup>Cl peak amplitude appears equivalent to that of the 459 Laschamp. Surprisingly, in Wagner et al. (2000b), smoothing of the dataset with a 1/3000 yrs<sup>-</sup> 460 <sup>1</sup> low-pass filter reduces the <sup>36</sup>Cl Mono Lake peak previously noted in Wagner et al. (2000a) 461 to the level of an insignificant variation. Together with this observation, the <sup>10</sup>Be fluxes in 462 Summit ice cores and the presented high-resolution <sup>10</sup>Be/<sup>9</sup>Be record question the validity of a 463 <sup>36</sup>Cl signature linked to the Mono Lake dipole field low. 464

Lal's algorithm (1988) has been used to convert the authigenic <sup>10</sup>Be/<sup>9</sup>Be record into a relative Virtual Dipole Moment (VDM) record that is compared to the GLOPIS-75 stacked paleomagnetic record (Fig. 6c). This reconstruction and the GLOPIS-75 curve agree relatively
well over the 30-48 ka time interval, although the cosmogenic record points out possible
higher intensities for the 20-30 ka period and beyond 48 ka than indicated in the
paleomagnetic records of the GLOPIS-75 stack.

#### 471 4.3 Reconstruction of the geomagnetic dipole moment variations from the ${}^{10}Be/{}^{9}Be$ ratios

#### 472 A stack of the Portuguese Margin $^{10}Be/^{9}Be$ records

In order to achieve a statistically significant record of the authigenic <sup>10</sup>Be/<sup>9</sup>Be ratio, 473 474 the MD04-2811 record was combined with the record previously obtained by Carcaillet et al. 475 (2004) on core MD95-2042, recovered at the same site. These data were relocated on the 476 depth scale of core MD04-2811 using the MS correlation matrix (reciprocal to the one used to 477 transfer chronological data (Fig. 7a)). Be ratios measured on both cores vary in a similar 478 range and present the same structure characterized both by a sharp maximum linked to the LE 479 dipole low and by the absence of any other significant peak. Differences between MD95-2042 480 and MD04-2811 data sets result from local sedimentary processes, differential postdepositional processes (i.e. compaction), sampling and analytical uncertainties. After stacking 481 the two <sup>10</sup>Be/<sup>9</sup>Be ratios records, a smoothed composite record was produced by computing 482 483 weighted moving averages over a 1000 years sliding window offset by 500 years (except for 484 the 20-25 ka interval, for which MD04-2811 data are directly reported). Associated 485 uncertainties combine both the sample analytical uncertainty and standard deviation around 486 each weighted average, and are calculated using the unbiased weighted estimator of the 487 sample variance (see Electronic Appendix Table A.2). Fig. 7b shows this composite record and the associated standard error (1 $\sigma$ ). The 1000 yrs-smoothed authigenic <sup>10</sup>Be/<sup>9</sup>Be composite 488 record displays a ~1.45 time increase during the LE time interval compared to the long-term 489 490 average  $(1.32 \times 10^{-8})$ . Although the studied time interval covers the age range of the Mono Lake Excursion, the slight increase of the <sup>10</sup>Be/<sup>9</sup>Be composite curve at ~33-34 ka is not 491 492 significant regarding the uncertainties associated with the adjacent data points. This reveals the absence of any <sup>10</sup>Be overproduction linked to a dipole reduction associated with the Mono 493 lake Excursion. This observation -if confirmed at other sites- would have strong implications 494 495 on the interpretation of the magnitude and duration of the "geomagnetic dipole low" 496 associated with the Mono lake Excursion.

#### 498 Calibrating to virtual dipole moments

499 The previously described <sup>10</sup>Be-stack was converted into Virtual Dipole Moment (VDM) variations using absolute paleointensities reconstructed from lava flows. In order to 500 reproduce the full range of the <sup>10</sup>Be production variation, the <sup>10</sup>Be/<sup>9</sup>Be ratios measured along 501 502 core MD04-2811 were associated with VDM values selected from the GEOMAGIA-50 503 (Korhonen et al., 2008) absolute paleointensity database (see Electronic Appendix Fig. A.3 and Table A.3). <sup>10</sup>Be production rates are inversely proportional to VDM values, thus (1) the 504  $^{10}$ Be/ $^{9}$ Be maximum value was assigned to the minimum VDM value linked to the LE, (2) the 505 intermediate <sup>10</sup>Be/<sup>9</sup>Be ratios were assigned to the intermediate VDM values, and (3) the 506 minimum <sup>10</sup>Be/<sup>9</sup>Be values were assigned to the maximum VDM values. 507

The relationship thus obtained between authigenic <sup>10</sup>Be/<sup>9</sup>Be ratios and VDMs is, at 508 best, fitted by a polynomial of order 2 (Fig. A.3). When applied to the  ${}^{10}\text{Be}/{}^{9}\text{Be}$  stack this 509 polynomial produces a "<sup>10</sup>Be-derived VDM" record for the 20-50 ka interval, which can be 510 compared to GLOPIS-75 and SINT-800 paleointensity stacks (Fig. 8). This <sup>10</sup>Be based VDM 511 512 record provides a reconstruction in better agreement with GLOPIS-75 than does Lal's 513 algorithm conversion (Fig. 6c). It documents a stronger geomagnetic moment before (maximum ~ $10.5 \times 10^{22}$  A.m<sup>2</sup>) than after (maximum ~ $7.0 \times 10^{22}$  A.m<sup>2</sup>) the LE, and allows to 514 estimate a decreasing rate of  $\sim 1 \times 10^{22}$  A.m<sup>2</sup>/ka for the dipole collapse which initiates the 515 Laschamp (minimum  $\sim 2.6 \times 10^{22}$  A.m<sup>2</sup> reached at  $\sim 41$  ka). Although this record exhibits the 516 same main variations as GLOPIS-75, it fails to reproduce a sharp VDM reduction at the age 517 of the Mono Lake Excursion: at 34-32 ka relatively low VDM values (~  $4.7 \times 10^{22}$  A.m<sup>2</sup>) are in 518 opposition with the sharp increase recorded at 32-33 ka in the GLOPIS-75. 519

520

#### 521 <u>5. Conclusion</u>

Authigenic <sup>10</sup>Be/<sup>9</sup>Be ratios measured along a rapidly accumulating sedimentary sequence from the North-East Atlantic (core MD04-2811) provide a new record of dipole geomagnetic moment variations over the 20-50 ka time interval, independent from paleomagnetic methodological constraints.

526 This first successful geomagnetic reconstruction using both authigenic  ${}^{10}\text{Be}/{}^{9}\text{Be}$  and 527  ${}^{10}\text{Be}/{}^{230}\text{Th}_{xs}$  normalization techniques of  ${}^{10}\text{Be}$  concentrations in marine sediments evidence an 528 almost doubling of the atmospheric  ${}^{10}\text{Be}$  production which documents the occurrence of the Laschamp geomagnetic dipole low prior to the Heinrich Event 4, at an age of ~ 41 ka. These ratios are fully compatible with the Summit ice core <sup>10</sup>Be record, which further supports their significance in terms of <sup>10</sup>Be atmospheric production. Identical <sup>10</sup>Be flux responses recorded in a polar ice core and in a mid-latitude marine core strongly suggest that the cosmogenic nuclide overproduction signal in Greenland ice results from the global geomagnetic moment modulation.

The authigenic <sup>10</sup>Be/<sup>9</sup>Be ratio records of neighboring cores MD04-2811 and MD95-535 536 2042 cores were compiled and averaged over a 1 ka sliding window. The obtained stack was 537 calibrated using absolute virtual dipole moment (VDM) values, determined from lava flow paleointensities, to provide a <sup>10</sup>Be derived VDM record. This allows to characterize the 538 Laschamp dipole low by a decrease from  $\sim 10.5 \times 10^{22}$  A.m<sup>2</sup> at  $\sim 49$  ka to  $\sim 2.6 \times 10^{22}$  A.m<sup>2</sup> at  $\sim 41$ 539 ka. The latter estimate is concordant with radiometric ages obtained on excursional lava 540 541 flows. This record fails to document a significant VDM reduction at the age of the Mono 542 Lake Excursion (32-34 ka).

By providing a new high-resolution <sup>10</sup>Be dataset at mid-latitude, the results presented 543 544 here are of great interest for better constraining the influence of geomagnetic field intensity 545 variations on cosmogenic nuclide production rates. Among these cosmogenic nuclides, atmospheric <sup>14</sup>C is of particular importance considering that the <sup>14</sup>C calibration curve lacks 546 547 accurate data during the time period covered by this study. Such new high-resolution datasets 548 from different latitudes are required to make significant advances in quantifying all processes involved in atmospheric  $\Delta^{14}$ C variations. Similarly, reconstructing past VDM variations is of 549 fundamental importance in quantifying in-situ cosmogenic nuclide production rate variations 550 551 and thus in accurately measuring Earth's surface processes. Further investigations, notably at 552 low-latitude sites where the shielding effect from the geomagnetic dipole field is maximized, 553 are currently underway.

- 554
- 555
- 556
- 557
- 558

#### 559 Acknowledgements:

560 This study was funded by the MAG-ORB project of the ANR (Agence Nationale de la 561 Recherche) program BLANC #ANR-09-BLAN-0053-01. The ASTER French AMS national 562 facility (CEREGE, Aix en Provence) is supported by the INSU/CNRS, the French Ministry of 563 Research and Higher Education, IRD and CEA. We gratefully thank Maurice Arnold, 564 Georges Aumaître and Karim Keddadouche for their invaluable help and support during the 565 AMS measurements, and Wulfran Barthelemy for his assistance during the TIMS 566 measurements. We are also grateful to Eva Moreno, for helping in U-channel sampling and in 567 preliminary paleomagnetic measurements, as well as R. Muscheler who kindly provided the <sup>10</sup>Be ice cores data. We acknowledge the scientific and technical crew of R.V. Marion 568 569 Dufresne cruise 140 who collected core MD04-2811. We thank Professor Martin Frank and 570 an anonymous reviewer who helped to improve this manuscript.

#### 571

#### 572 **References:**

573

Andersen, K.K., Svensson, A., Rasmussen, S.O., Steffensen, J.P., Johnsen, S.J., Bigler, M.,
Röthlisberger, R., Ruth, U., Siggaard-Andersen, M.-L., Dahl-Jensen, D., Vinther, B.M.,
Clausen, H.B., 2006. The Greenland Ice Core Chronology 2005, 15–42 ka. Part 1:
constructing the time scale. Quat. Sci. Rev. 25, 246-257.

578

Andersen, M.B., Stirling, C.H., Potter, E.-K., Halliday, A.N., 2004. Toward epsilon levels of
 measurement precision on <sup>234</sup>U/<sup>238</sup>U by using MC-ICPMS. Int. J. of Mass Spectrom. 237,
 107-118.

582

Andersen, M.B., Stirling, C.H., Zimmermann, B., Halliday, A.N., 2010. Precise determination
of the open ocean <sup>234</sup>U/<sup>238</sup>U composition. Geochem., Geophys., Geosyst. 11, Q12003, doi:
10.1029/2010GC003318.

587	Baas, J.H., Mienert, J., Abrantes, F., Prins, M.A., 1997. Late Quaternary sedimentation on the							
588	Portuguese	continental	margin:	climate-related	processes	and	products.	Palaeogeogr.,
589	Palaeoclimatol., Palaeoecol. 130, 1-23.							

590

Bacon, M.P., 1984. Glacial to interglacial changes in carbonate and clay sedimentation in the
 Atlantic Ocean estimated from <sup>230</sup>Th measurements. Isot. Geosci. 2, 97-111.

593

Bard, E., Arnold, M., Maurice, P., Duprat, J., Moyes, J., Duplessy, J.-C., 1987. Retreat
 velocity of the North Atlantic polar front during the last deglaciation determined by <sup>14</sup>C
 accelerator mass spectrometry. Nature 328, 791-794.

597

Bard, E., Hamelin, B., Fairbanks, R.G., Zindler, A., Mathieu, G., Arnold, M., 1990. U/Th and
 <sup>14</sup>C ages of corals from Barbados and their use for calibrating the <sup>14</sup>C time scale beyond 9000
 years BP. Nucl. Instr. Meth. in Phys. Res. B-52, 461-468.

601

Bard, E., Rostek, F., Turon, J.-L., and Gendreau, S., 2000. Hydrological Impact of Heinrich
Events in the Subtropical Northeast Atlantic. Science 289, 1321-1324.

604

- Bard, E., Rostek, F., Ménot-Combes, G., 2004. Radiocarbon calibration beyond 20,000 <sup>14</sup>C yr
- B.P. by means of planktonic foraminifera of the Iberian Margin. Quat. Res. 61, 204-214.
- 607
- Baroni, M., Bard, E., Petit, J.R., Magnan, O., Bourlès, D.L., 2011. Volcanic and solar activity,
  and atmospheric circulation influences on cosmogenic <sup>10</sup>Be fallout at Vostok and Concordia
  (Antarctica) over the last 60 years. Geochim. Cosmochim. Acta, ISSN 0016-7037, doi:
  10.1016/j.gca.2011.09.002.

613 614	Benson, L., Liddicoat, J., Smoot, J., Sarna-Wojcicki, A., Negrini, R., Lund, S., 2003. Age of the Mono Lake excursion and associated tephra. Quat. Sci. Rev. 22, 135-140.
615	
616 617	Bonhommet, N., Babkine, J., 1967. Sur la présence d'aimantations inverses dans la Chaîne des Puys — Massif Central, France. C.R.A.S. Paris 264, 92.
618	
619 620	Bourlès, D., Raisbeck, G.M., Yiou, F., 1989. <sup>10</sup> Be and <sup>9</sup> Be in marine sediments and their potential for dating. Geochim. Cosmochim. Acta 53, 443-452.
621	
622 623	Brown, E.T., Measures, C.I., Edmond, J.M., Bourlès, D.L., Raisbeck, G.M., Yiou, F., 1992. Continental inputs of beryllium to the oceans. Earth Planet. Sci. Lett. 114, 101-111.
624	
625 626	Carcaillet, J., Thouveny, N., Bourlès, D.L., 2003. Geomagnetic moment instability between 0.6 and 1.3 Ma from cosmonuclide evidence. Geophys. Res. Lett. 30, 1792.
627	
628 629 630	Carcaillet, J., Bourlès, D.L., N.Thouveny, 2004a. Geomagnetic dipole moment and <sup>10</sup> Be production rate intercalibration from authigenic <sup>10</sup> Be/ <sup>9</sup> Be for the last 1.3 Ma. Geochem. Geophys. Geosyst. 5, 397-412, Q05006, doi: 10.1029/2003GC000641.
631	
632 633 634	Carcaillet, J., Bourlès, D.L., Thouveny, N., Arnold, M., 2004b. A high resolution authigenic <sup>10</sup> Be/ <sup>9</sup> Be record of geomagnetic moment variations over the last 300 ka from sedimentary cores of the Portuguese margin. Earth Planet. Sci. Lett. 219, 397-412.
635	
636 637	Cassata, W.S., Singer, B.S., Cassidy, J., 2008. Laschamp and Mono Lake geomagnetic excursions recorded in New Zealand. Earth Planet. Sci. Lett. 268, 76-88.
638	

Channell, J., 2006. Late Brunhes polarity excursions (Mono Lake, Laschamp, Iceland Basin
and Pringle Falls) recorded at ODP Site 919 (Irminger Basin). Earth Planet. Sci. Lett. 244,
378-393.

642

Chase, Z., Anderson, R.F., Fleisher, M.Q., Kubik, P.W., 2002. The influence of particle
composition and particle flux on scavenging of Th, Pa and Be in the ocean. Earth Planet. Sci.
Lett. 204, 215-229.

646

Chmeleff, J., von Blanckenburg, F., Kossert, K., Jakob, D., 2010. Determination of the <sup>10</sup>Be
half-life by multicollector ICP-MS and liquid scintillation counting. Nuclear Instruments and
Methods in Physics Research Section B: Beam Interactions with Materials and Atoms 268,
192-199.

651

Christl, M., Strobl, C., Mangini, A., 2003. Beryllium-10 in deep-sea sediments: a tracer for
the Earth's magnetic field intensity during the last 200,000 years. Quat. Sci. Rev. 22, 725-739.

654

Christl, M., Mangini, A., Kubik, P.W., 2007. Highly resolved Beryllium-10 record from ODP
Site 1089--A global signal? Earth Planet. Sci. Lett. 257, 245-258.

657

658 Christl, M., Lippold, J., Steinhilber, F., Bernsdorff, F., Mangini, A., 2010. Reconstruction of 659 global <sup>10</sup>Be production over the past 250 ka from highly accumulating Atlantic drift 660 sediments. Quat. Sci. Rev. 29, 2663-2672.

661

Coe, R.S., Liddicoat, J.C., 1994. Overprinting of natural magnetic remanence in lake
sediments by subsequent high intensity field. Nature 367, 57-59.

Denham, C.R., Cox, A., 1971. Evidence that the Laschamp polarity event did not occur
13300–30400 years ago. Earth Planet. Sci. Lett. 13, 181-190.

667

Deschamps, P., Doucelance, R., Ghaleb, B., Michelot, J.L., 2003. Further investigations on
optimized tail correction and high-precision measurement of Uranium isotopic ratios using
Multi-Collector ICP-MS. Chem. Geol. 201, 141-160.

671

Deschamps, P., Hillaire-Marcel, C., Michelot, J.L, Doucelance, R., Ghaleb, B., Buschaert, S.,
2004. <sup>234</sup>U/<sup>238</sup>U Disequilibrium along stylolitic discontinuities in deep Mesozoic limestone
formations of the Eastern Paris basin: evidence for discrete uranium mobility over the last 1-2
million years. Hydrol. Earth Syst. Sci. 8, 35-46.

676

Deschamps, P., Durand, N., Bard, E., Hamelin, B., Camoin, G., Thomas, A.L., Henderson,
G.M., Okuno, J., Yokoyama, Y., Submitted. Dramatic ice sheet collapse 14,600 years ago at
onset of Bølling warming. Nature.

680

Elsasser, W., Ney, E.P., Winckler, J.R., 1956. Cosmic-ray intensity and geomagnetism.
Nature 178, 1226-1227.

683

Finkel, R.C., Nishiizumi, K., 1997. Beryllium 10 concentrations in the Greenland Ice Sheet
Project 2 ice core from 3–40 ka. J. Geophys. Res. 102 26699-26706.

686

François, R., Frank, M., Rutgers van der Loeff, M.M., Bacon, M.P., 2004. <sup>230</sup>Th
normalization: An essential tool for interpreting sedimentary fluxes during the late
Quaternary. Paleoceanography 19, 10-18.

Frank, M., Schwarz, B., Baumann, S., Kubik, P.W., Suter, M., Mangini, A., 1997. A 200 kyr
 record of cosmogenic radionuclide production rate and geomagnetic field intensity from <sup>10</sup>Be
 in globally stacked deep-sea sediments. Earth Planet. Sci. Lett. 149, 121-129.

694

Frank, M., 2000. Comparison of cosmogenic radionuclide production and geomagnetic fieldintensity over the last 200,000 years. Phil. Trans. R. Soc. Lond. A 358, 1089-1107.

697

- Guillou, H., Singer, B.S., Laj, C., Kissel, C., Scaillet, S., Jicha, B.R., 2004. On the age of the
  Laschamp geomagnetic excursion. Earth Planet. Sci. Lett. 227, 331-343.
- Guyodo, Y., Valet, J.P., 1999. Global changes in intensity of the Earth's magnetic field during
- 701 the past 800 kyr. Nature 399, 249-252.

702

Hall, I.R., McCave, I.N., 2000. Palaeocurrent reconstruction, sediment and thorium focussing
on the Iberian margin over the last 140 ka. Earth Planet. Sci. Lett. 178, 151-164.

705

Henderson, G.M., Anderson, R.F., 2003. The U-series toolbox for paleoceanography,. Rev.
Mineral. Geochem. 52, 493-531.

708

Henken-Mellies, W.U., Beer, J., Heller, F., Hsü, K.J., Shen, C., Bonani, G., Hofmann, H.J.,
Suter, M., Wölfli, W., 1990. <sup>10</sup>Be and <sup>9</sup>Be in South Atlantic DSDP Site 519: Relation to
geomagnetic reversals and to sediment composition. Earth Planet. Sci. Lett. 98, 267-276.

712

Kent, D.V., Hemming, S.R., Turrin, B.D., 2002. Laschamp Excursion at Mono Lake? Earth
Planet. Sci. Lett. 197, 151-164.

- Knudsen, M.F., Henderson, G.M., Frank, M., Mac Niocaill, C., Kubik, P.W., 2008. In-phase
  anomalies in Beryllium-10 production and palaeomagnetic field behaviour during the Iceland
  Basin geomagnetic excursion. Earth Planet. Sci. Lett. 265, 588-599.
- 719
- Kissel, C., Laj, C., Labeyrie, L., Dokken, T., Voelker, A., Blamart, D., 1999. Rapid climatic
  variations during marine isotopic stage 3: magnetic analysis of sediments from Nordic Seas
  and North Atlantic. Earth Planet. Sci. Lett. 171, 489-502.
- 723

Korhonen, K., Donadini, F., Riisager, P., Pesonen, L., 2008. GEOMAGIA50: an
archeointensity database with PHP and MySQL. Geochem. Geophys. Geosyst. 9 (4), Q04029,
doi: 10.1029/2007GC001893

727

Korschinek, G., Bergmaier, A., Faestermann, T., Gerstmann, U.C., Knie, K., Rugel, G.,
Wallner, A., Dillmann, I., Dollinger, G., von Gostomski, C.L., Kossert, K., Maiti, M.,
Poutivtsev, M., Remmert, A., 2010. A new value for the half-life of <sup>10</sup>Be by Heavy-Ion
Elastic Recoil Detection and liquid scintillation counting. Nucl. Instr. Meth. in Phys. Res.
Sect. B: Beam Interact. Mater. At. 268, 187-191.

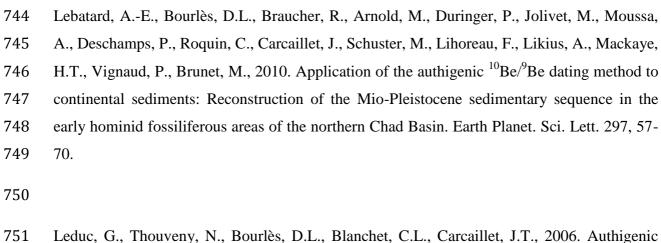
733

- Kristjansson, L., Gudmundsson, A.A., 1980. Geomagnetic excursions in late-glacial basalt
  outcrop in south-western Iceland. Geophys. Res. Lett.7, 337–340.
- 736
- Laj, C., Kissel, C., Beer, J., 2004. High resolution global paleointensity stack since 75 kyr
  (GLOPIS-75) calibrated to absolute values. In: Channell, J.E.T., Kent, D.V., Lowrie, W.,
  Meert, J.G. (Eds.), Timescales of the Paleomagnetic Field. . Geophys. Monogr. 145.

740

Lal, D., 1988. Theoretically expected variations in the terrestrial cosmic-ray production rates
of isotopes. Soc. Italia. di Fisica-Bologna-Italy XCV corso, 216-233.

743



<sup>751</sup> Leduc, G., Thouveny, N., Bourles, D.L., Blanchet, C.L., Carcallet, J.I., 2006. Authigenic
 <sup>752</sup> <sup>10</sup>Be/<sup>9</sup>Be signature of the Laschamp excursion: A tool for global synchronisation of
 <sup>753</sup> paleoclimatic archives. Earth Planet. Sci. Lett. 245, 19-28.

754

Levi, S., Gudmunsson, H., Duncan, R.A., Kristjansson, L., Gillot, P.V., Jacobsson, S.P.,
1990. Late Pleistocene geomagnetic excursion in Icelandic lavas: Confirmation of the
Laschamp excursion. Earth Planet. Sci. Lett. 96, 443–457.

758

Liddicoat, J.C., 1992. Mono Lake Excursion in Mono Basin, California, and at Carson Sinkand Pyramid Lake, Nevada. Geophys. J. Intern. 108, 442-452.

761

765

Masarik, J., Beer, J., 1999. Simulation of particle fluxes and cosmogenic nuclide production
in the Earth's atmosphere. J. Geophys. Res. 104, 12099-12111.

<sup>Lund, S.P., Schwartz, M., Keigwin, L., Johnson, T., 2005. Deep-sea sediment records of the
Laschamp geomagnetic field excursion (<41,000 calendar years before present. J. Geophys.</li>
Res. 110, Q12006.</sup> 

Monaghan, M.C., Krishnaswami, S., Turekian, K.K., 1986. The global-average production
rate of <sup>10</sup>Be. Earth Planet. Sci. Lett. 76, 279-287.

771

Moreno, E., Thouveny, N., Delanghe, D., McCave, I.N., Shackleton, N.J., 2002. Climatic and
oceanographic changes in the Northeast Atlantic reflected by magnetic properties of
sediments deposited on the Portuguese Margin during the last 340 ka. Earth Planet. Sci. Lett.
202, 465-480.

776

Muscheler, R., Beer, J., Wagner, G., Laj, C., Kissel, C., Raisbeck, G.M., Yiou, F., Kubik,
P.W., 2004. Changes in the carbon cycle during the last deglaciation as indicated by the
comparison of <sup>10</sup>Be and <sup>14</sup>C records. Earth Planet. Sci. Lett. 219, 325-340.

780

Muscheler, R., Beer, J., Kubik, P.W., Synal, H.A., 2005. Geomagnetic field intensity during
the last 60,000 years based on <sup>10</sup>Be and <sup>36</sup>Cl from the Summit ice cores and <sup>14</sup>C. Quat. Sci.
Rev. 24, 1849-1860.

784

Negrini, R.M., Davis, J.O., Verosub, K.L., 1984. Mono Lake geomagnetic excursion found at
Summer Lake, Oregon. Geology 12, 643-646.

787

Negrini, R., Erbes, K.F., Herrera, A.M., Roberts, A.P., Cohen, A., Palacios-Fest, M., Wigand,
P.E., Foit, F., 2000. A paleoclimate record for the past 250,000 years from Summer Lake,
Oregon, USA: I. Age control and magnetic lake level proxies. J. Paleolimn. 24, 125-149.

791

- Nishiizumi, K., Imamura, M., Caffee, M.W., Southon, J.R., Finkel, R.C., McAninch, J., 2007.
- Absolute calibration of <sup>10</sup>Be AMS standards. Nucl. Instr. Meth. in Phys. Res. Sect. B: Beam
- 794 Interact. Mater. At. 258, 403-413.

NGRIP-dating-group, 2006. Greenland Ice Core Chronology 2005 (GICC05). IGBP
PAGES/World Data Center for Paleoclimatology Data Contribution Series # 2006-118.
NOAA/NCDC Paleoclimatology Program, Boulder CO, USA.

799

NGRIP-Members, 2004. High-resolution record of Northern Hemisphere climate extending
into the last interglacial period. Nature 431, 147–151.

802

Nowaczyk, N.R., Knies, J., 2000. Magnetostratigraphic results from the eastern Arctic ocean:
 AMS <sup>14</sup>C ages and relative paleointensity data of the mono lake and Laschamp geomagnetic
 reversal excursions. Geophys. J. Intern. 140, 185-197.

806

Paillard, D., Labeyrie, L., Yiou, P., 1996. Macintosh program performs time-series analysis.
Eos Trans. AGU 77, 379.

809

Pailler, D., Bard, E., 2002. High frequency palaeoceanographic changes during the past 140
000 yr recorded by the organic matter in sediments of the Iberian Margin. Palaeogeogr.
Palaeoclimatol. Palaeoecol. 181, 431-452.

813

- Plenier, G., Valet, J.-P., Guérin, G., Lefêvre, J.-C., LeGoff, M., Carter-Stiglitz, B., 2007.
  Origin and age of the directions recorded during the Laschamp event in the Chaîne des Puys
  (France). Earth Planet. Sci. Lett. 259, 414-431.
- 817
- Raisbeck, G.M., Yiou, F., Fruneau, M., Loiseaux, J.M., Lieuvin, M., Ravel, J.C., 1981.
  Cosmogenic Be-10/Be-7 as a probe of atmospheric transport processes. Geophys. Res. Lett.
  8, 1015-1018.

- Raisbeck, G.M., Yiou, F., Jouzel, J., Stocker, T.F., 2007. Direct north-south synchronization
  of abrupt climate change record in ice cores using Beryllium 10. Climate of the Past 3, 541547.
- 825
- Rasmussen, S.O., Seierstad, I.K., Andersen, K.K., Bigler, M., D. Dahl-Jensen, S.J. Johnsen,
  2006. NGRIP, GRIP, and GISP2 Synchronization Match Points. IGBP PAGES/World Data
  Center for Paleoclimatology. Data Contribution Series # 2006-120. NOAA/NCDC
  Paleoclimatology Program, Boulder CO, USA.
- 830
- Reimer, P.J., Baillie, M.G.L., Bard, E., Bayliss, A., Beck, J.W., Blackwell, P.G., Bronk
  Ramsey, C., Buck, C.E., Burr, G.S., Edwards, R.L., Friedrich, M., Grootes, P.M., Guilderson,
  T.P., Hajdas, I., Heaton, T.J., Hogg, A.G., Hughen, K.A., Kaiser, K.F., Kromer, B.,
  McCormac, G., Manning, S., Reimer, R.W., Richards, D.A., Southon, J.R., Talamo, S.,
  Turney, C.S.M., van der Plicht, J., Weyhenmeyer, C.E., 2009. IntCal09 and Marine09
- radiocarbon age calibration curves, 0-50000 Years cal BP. Radiocarbon 51, 1111-1150.
- 837
- Robinson, C., Raisbeck, G.M., Yiou, F., Lehman, B., Laj, C., 1995. The relationship between
   <sup>10</sup>Be and geomagnetic field strength records in central North Atlantic sediments during the
   last 80 ka. Earth Planet. Sci. Lett. 136, 551-557.
- 841
- 842 Shackleton, N.J., Fairbanks, R.G., Chiu, T.-C., Parrenin, F., 2004. Absolute calibration of the 843 Greenland time scale: implications for Antarctic time scales and for  $\delta^{14}$ C. Quat. Science Rev. 844 23, 1513-1522.
- 845
- Singer, B.S., Guillou, H., Jicha, B.R., Laj, C., Kissel, C., Beard, B.L., Johnson, C.M., 2009.
  <sup>40</sup>Ar/<sup>39</sup>Ar, K-Ar and <sup>230</sup>Th-<sup>238</sup>U dating of the Laschamp Excursion: A radioisotopic tie-point for ice core and climate chronologies. Earth Planet. Sci. Lett. 286, 80-88.
- 849
- 850 Skinner, L.C., and McCave, I.N., 2003. Analysis and modelling of gravity- and piston coring851 based on soil mechanics. Mar. Geol. 199, 181-204.
- 852
- 853 Svensson, A., Andersen, K.K., Bigler, M., Clausen, H.B., Dahl-Jensen, D., Davies, S.M.,
- Johnsen, S.J., Muscheler, R., Parrenin, F., Rasmussen, S.O., Röthlisberger, R., Seierstad, I.,

- Steffensen, J.P., Vinther, B.M., 2008. A 60 000 year Greenland stratigraphic ice corechronology. Climate of the Past 4, 47-57.
- 857
- Széréméta, N., Bassinot, F., Balut, Y., Labeyrie, L., Pagel, M., 2004. Oversampling of
  sedimentary series collected by giant piston corer: Evidence and corrections based on 3.5-kHz
  chirp profiles. Paleoceanography *19*, PA1005, doi: 10.1029/2002PA000795.
- 861
- Taylor, J.R., 1997. An Introduction to Error Analysis. The study of Uncertainties in Physical
  Measurements, Second ed., University Science Books, Sausalito, USA.
- 864
- Thomson, J., Nixon, S., Summerhayes, C.P., Schönfeld, J., Zahn, R., Grootes, P., 1999.
  Implications for sedimentation changes on the Iberian margin over the last two
  glacial/interglacial transitions from (<sup>230</sup>Th<sub>excess</sub>)<sub>0</sub> systematics. Earth Planet. Sci. Lett. 165, 255270.
- 869
- Thouveny, N., Creer, K.M., 1992. On the brievity of the Laschamp Excursion. Bull. Soc.
  Géol. Fr. 6, 771–780.
- 872
- Thouveny, N., Moreno, E., Delanghe, D., Candon, L., Lancelot, Y., Shackleton, N.J., 2000.
  Rock magnetic detection of distal ice-rafted debries: clue for the identification of Heinrich
  layers on the Portuguese margin. Earth Planet. Sci. Lett. 180, 61-75.
- 876
- Thouveny, N., Carcaillet, J., Moreno, E., Leduc, G., Nérini, D., 2004. Geomagnetic moment
  variation and paleomagnetic excursions since 400 kyr BP: a stacked record from sedimentary
  sequences of the Portuguese margin. Earth Planet. Sci. Lett. 219, 377-396.
- 880
- Thouveny, N., Bourlès, D.L., Saracco, G., Carcaillet, J.T., Bassinot, F., 2008. Paleoclimatic
  context of geomagnetic dipole lows and excursions in the Brunhes, clue for an orbital
  influence on the geodynamo? Earth Planet. Sci. Lett. 275, 269-284.
- 884
- Vlag, P., Thouveny, N., Williamson, D., Rochette, P., Ben-Atig, F., 1996. Evidence for a
  geomagnetic excursion recorded in the sediments of Lac St. Front, France: a link with the
  Laschamp Excursion? J. Geophys. Res. 101, 28211–28230.
- 888

- Wagner, G., Beer, J., Laj, C., Kissel, C., Masarik, J., Muscheler, R., Synal, H.A., 2000a.
  Chlorine-36 evidence for the Mono Lake event in the Summit GRIP ice core. Earth Planet.
  Sci. Lett. 181, 1-6.
- 892
- 893 Wagner, G., Masarik, J., Beer, J., Baumgartner, S., Imboden, D., Kubik, P.W., Synal, H.A.,
- 894 Suter, M., 2000b. Reconstruction of the geomagnetic field between 20 and 60 kyr BP from
- 895 cosmogenic radionuclides in the GRIP ice core. Nuclear Instruments and Methods in Physics
- Research Section B: Beam Interactions with Materials and Atoms 172, 597-604.
- 897
- Wang, Y.J., Cheng, H., Edwards, R.L., An, Z.S., Wu, J.Y., Shen, C.-C., and Dorale, J.A.,
  2001. A High-Resolution Absolute-Dated Late Pleistocene Monsoon Record from Hulu Cave,
- 900 China Science 294, 2345-2348.
- 901
- 902 Yiou, F., Raisbeck, G.M., Baumgartner, S., Beer, J., Hammer, C., Johnsen, S., Jouzel, J.,
- Kubik, P.W., Lestringuez, J., Stiévenard, M., Sutter, M., Yiou, P., 1997. Beryllium 10 in the
  Greenland Ice Core Project ice core at Summit, Greenland. J. Geophys. Res. 102, 2678326794.
- 906
- 207 Zimmerman, S.H., Hemming, S.R., Kent, D.V., Searle, S.Y., 2006. Revised chronology for
  208 late Pleistocene Mono Lake sediments based on paleointensity correlation to the global
  209 reference curve. Earth Planet. Sci. Lett. 252, 94-106.
- 910
- 911
- 912
- 913
- . .
- 914
- 915
- 916

917 **Figure Captions :** 918 919 "The Laschamp geomagnetic dipole low expressed as a cosmogenic <sup>10</sup>Be atmospheric 920 overproduction at ~41 ka." 921 By L. Ménabréaz \*, N. Thouveny, D.L. Bourlès, P. Deschamps, B. Hamelin and F. Demory. 922 \* corresponding author: menabreaz@cerege.fr 923 Revised version submitted to Earth and Planetary Science Letters 924 Fig. 1. Location map of the studied MD04-2811 core. Other cores cited in the text 925 (MD95-2042 and SU81-18 were recovered at the same site. Fig. 2. Magnetic properties and cosmogenic nuclide <sup>10</sup>Be record as a function of depth in core 926 927 MD04-2811. (a) Magnetic susceptibility; susceptibility peaks identify distal ferrimagnetic 928 IRD layers deposited during Heinrich Events 1 to 5 (labeled H1 to H5). (b) Relative paleointensity (NRM/ARM ratios at 30mT alternating field step). (c) Authigenic <sup>10</sup>Be/<sup>9</sup>Be 929 ratios (10<sup>-8</sup>) with 1 $\sigma$  uncertainty. Solid and dotted lines correspond to the mean value over the 930 931 20-50 ka time period and the associated standard deviation  $(1\sigma)$ , respectively (see Table 1). 932 Fig. 3. (a-b) Paleoclimatic variations over Greenland and the Portuguese margin: (a)

933 variations of the air paleotemperature proxy over Greenland:  $\delta^{18}$ O of the NGRIP ice core 934 (NGRIP-Members, 2004 and references therein) plotted on the GICC05 time-scale (NGRIP 935 dating group, 2006 and references therein); (b) variations of the Portuguese margin sea-936 surface paleotemperature proxy: UK'37 alkenone index in core MD95-2042 (raw data of 937 Pailler and Bard, 2002) on a time scale tuned to NGRIP  $\delta^{18}$ O using the Analyserie software 938 (Paillard et al., 1996). Correlation tie-points are marked by vertical dashes. Triangles indicate 939 the position of the 23 samples used for AMS dating: raw data (Electronic Appendix, Table 940 A.1), are from Bard et al., 2004 and Shackleton et al., 2004); (c-d) Magnetic Susceptibility 941 (MS) records of Portuguese margin cores as a function of depth: (c) core MD95-2042 (specific MS in 10<sup>-9</sup> m<sup>3</sup>/kg) (data from Thouveny et al., 2000 transferred on the NGRIP 942 chronology; (d) core MD04-2811 (volume susceptibility 10<sup>-5</sup> SI). Susceptibility peaks (S0 to 943 944 S5) mark IRD layers deposited during the Younger Dryas (YD) and Heinrich events (H1 to 945 H5) events.

**Fig. 4.** Age-depth relationship in core MD04-2811. Open circles stand for the age model derived from the GICC05 chronology: the MD95-2042 age control obtained tuning UK'37 alkenone index and NGRIP  $\delta^{18}$ O (see Fig.3) was applied to core MD04-2811 by correlation of MS profiles using the Analyserie software (Paillard et al., 1996). Ages of the MD04-2811 susceptibility peaks (grey bands, ages reported on the left) are undistinguishable from ages of Heinrich layers computed by Thouveny et al. (2000): H2: 24778±297 yr BP; H3: 31163±509 yr BP; H4: 39379±948 yr BP.

- **Fig. 5.** (a) Downcore variation of the  ${}^{230}$ Th<sub>xs</sub>-normalized  ${}^{10}$ Be fluxes and (b) relation with authigenic  ${}^{10}$ Be/ ${}^{9}$ Be ratios measured on the same homogenized sediment samples.
- Fig. 6. (a and b) Relative temporal variations of <sup>10</sup>Be atmospheric production rate proxies 955 over the 20-50 ka interval. All records are normalized to their respective mean values over the 956 studied time interval. (a) Black dots represent the authigenic <sup>10</sup>Be/<sup>9</sup>Be record and the 957 associated  $1\sigma$  uncertainty. Grey dots represent the <sup>230</sup>Th<sub>xs</sub>-normalized <sup>10</sup>Be fluxes. (b) Black 958 dots represent the authigenic  ${}^{10}\text{Be}/{}^{9}\text{Be}$  record and the associated  $1\sigma$  uncertainty, and grey line 959 represents the Greenland <sup>10</sup>Be flux in Summit ice cores on GICC05 time scale (Finkel et al., 960 961 1997; Yiou et al., 1997; composite GRIP-GISP2: Muscheler et al., 2005). (c) Relative 962 temporal variations of geomagnetic field intensity over the 20-50 ka interval. Solid lines 963 represents the  $1\sigma$  uncertainty envelop of the GLOPIS-75 stack: raw data from Laj et al. (2004) are normalized to  $8 \times 10^{22}$  A.m<sup>2</sup> (most recent GLOPIS VADM value) and plotted on 964 965 the GICC05 time scale using the NGRIP, GRIP and GISP2 synchronization match points dataset (Rasmussen et al., 2006). Dots are the authigenic <sup>10</sup>Be/<sup>9</sup>Be-derived VDM record 966  $(M/M_0)$  calculated using the Lal's algorithm (1988):  $P/P_0 = (M/M_0)^{-0.5}$ , where  $P/P_0$  is the 967 authigenic  ${}^{10}\text{Be}/{}^9\text{Be}$  ratio divided by the surface sample value of  $(1.36\pm0.35)\times10^{-8}$ , 968 undistinguishable within uncertainties from the long-term average  $(1.44 \pm 0.043) \times 10^{-8}$ . 969
- **Fig. 7.** (a) Authigenic <sup>10</sup>Be/<sup>9</sup>Be ratios measured along MD04-2811 (solid circles) and MD95-2042 cores (open circle, Carcaillet et al., 2004) on the MD04-2811 depth scale. (b) Calculated authigenic <sup>10</sup>Be/<sup>9</sup>Be composite record over the 20-50 ka interval. This record is low-pass filtered (1/1000 yr<sup>-1</sup>). Associated uncertainties are  $1\sigma$ .

**Fig. 8.** Geomagnetic dipole moment variation during the 20-50 ka interval. The black curve is the Virtual Axial Dipole Moment (VADM) variations reconstructed from SINT800 (Guyodo and Valet, 1999). The grey zone is the  $1\sigma$  envelop of the GLOPIS-75 based VADM

- 977 reconstruction (Laj et al., 2004). Bold black curve is the authigenic <sup>10</sup>Be/<sup>9</sup>Be-based VDM
- 978 (Virtual Dipole Moment) record and  $1\sigma$  associated uncertainties.

- Highligths to the manuscript: "The Laschamp geomagnetic dipole low expressed as a
   cosmogenic <sup>10</sup>Be atmospheric overproduction at ~41 ka."
- 983
  984 by L. Ménabréaz \*, N. Thouveny, D.L. Bourlès, P. Deschamps, B. Hamelin and F. Demory.
  985 *Earth and Planetary Science Letters*
- $\Box$  Cosmogenic<sup>10</sup>Be concentration was measured along a marine sediment core (20 50ka)
- $\Box$  Authigenic<sup>9</sup>Be and excess <sup>230</sup>Th were used to normalize <sup>10</sup>Be concentrations
- $\Box$  A doubling of the cosmogenic production is revealed at ~41ka (NGRIP age)
- 990 Geomagnetic field intensity variations are reconstructed from <sup>10</sup>Be production rates
- $\Box$  The dipole low of Laschamp excursion is confirmed at 41 ka.